Supporting Information

3D-composite structure of FeP nanorods supported by vertical aligned graphene for high-performance hydrogen evolution reaction

Dongqi Li, Qingyu Liao, Bowen Ren, Qiuyan Jin, Hao Cui *, Chengxin Wang*

State Key Laboratory of Optoelectronic Materials and Technologies, School of Materials Science and Engineering, The Key Laboratory of Low-Carbon Chemistry & Energy Conservation of Guangdong Province, Sun Yat-Sen (Zhongshan)University, Guangzhou 510275, China

*Corresponding author: Fax: +86-20-8411-3901; e-mail: wchengx@mail.sysu.edu.cn; cuihao3@mail.sysu.edu.cn.

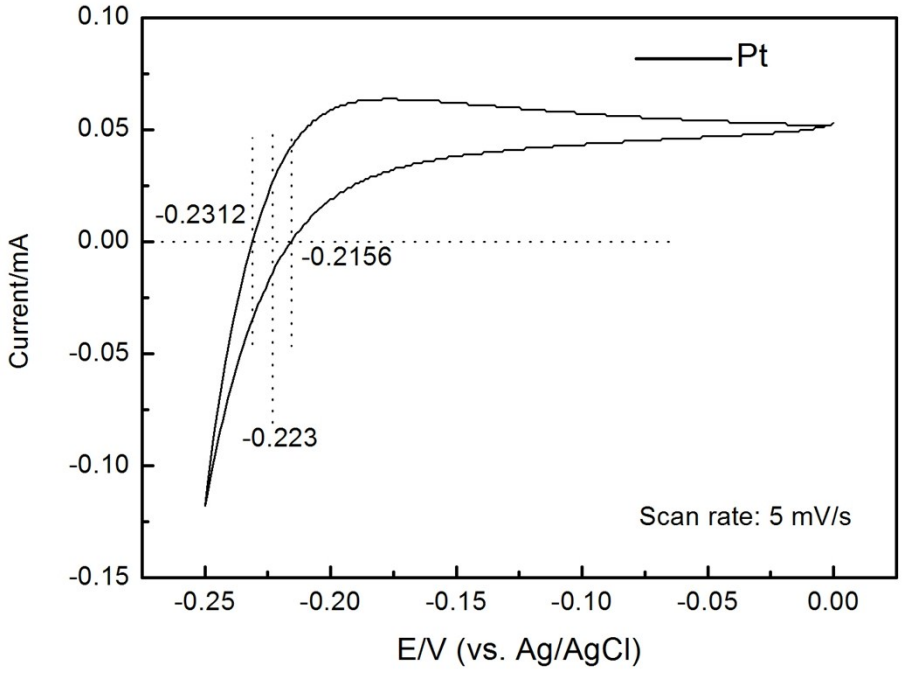

Fig. S1. RHE voltage calibration. The calibration was carried out in the high purity hydrogen saturated electrolyte with a Pt wire as the working electrode. The current-voltage scans were run at a scan rate of 5 mV/s, and the average of the two potentials at which the current crossed zero was taken to be the thermodynamic potential for the hydrogen electrode reactions. Our result shows that the E (Ag/AgCl) is lower than E (RHE) by 0.223V. This value is corresponding with the value 0.227V estimated from Nerst equation. The pH value is 0.34 for an 0.5 M H_2SO_4 solution and the E (RHE) = E (Ag/AgCl) +0.207+0.059 pH = E (Ag/AgCl) + 0.227.

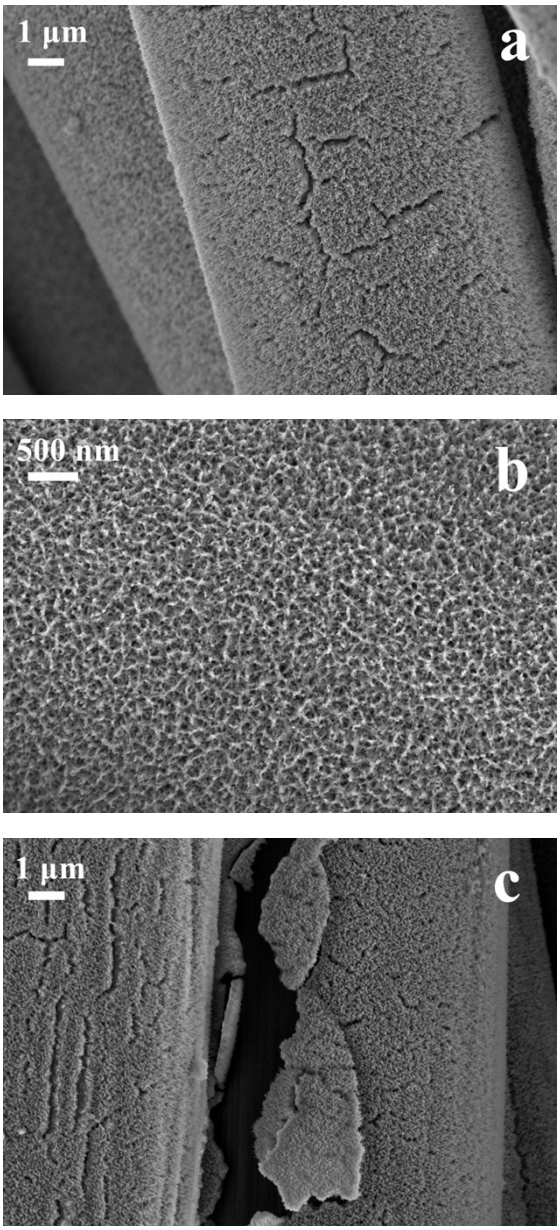

Fig. S2. Low-(a,c) and high-magnification (b) SEM images of FePNRs/CC.

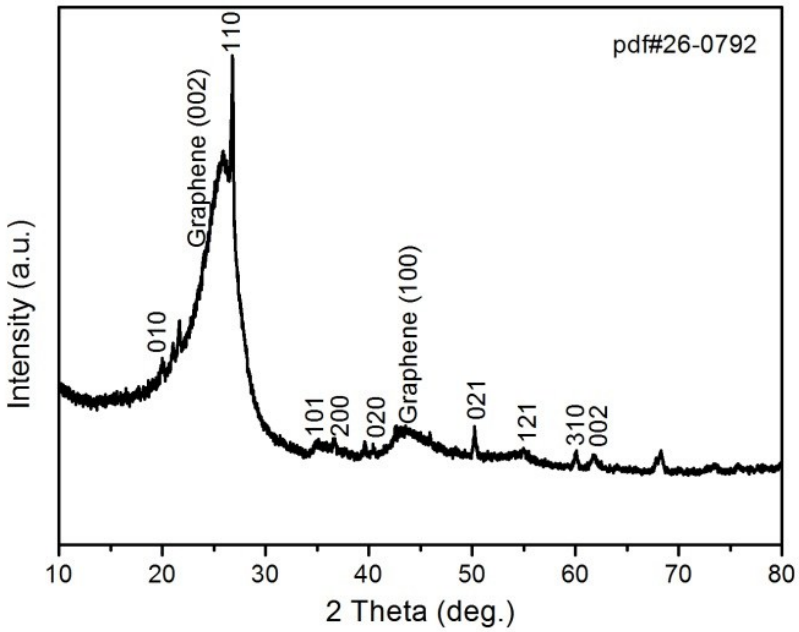

Fig. S3. The XRD pattern of FeOOH/VAGNs/CC with the label of standard crystallographic spectrum of FeOOH (pdf#26-0792).

Table S1. The atomic percentage measure by XPS

	Fe (%)	P (%)	C (%)	O (%)
Sample 1	8.57	16.39	20.94	54.1
Sample 2	6.1	13.88	49.49	30.53
Sample 3	9.29	14.27	28.49	47.95
Average	7.99	14.84	32.97	44.19

Noted: The average atomic ratio is Fe: P: C: O= 1: 1.85: 4.12: 5.53.

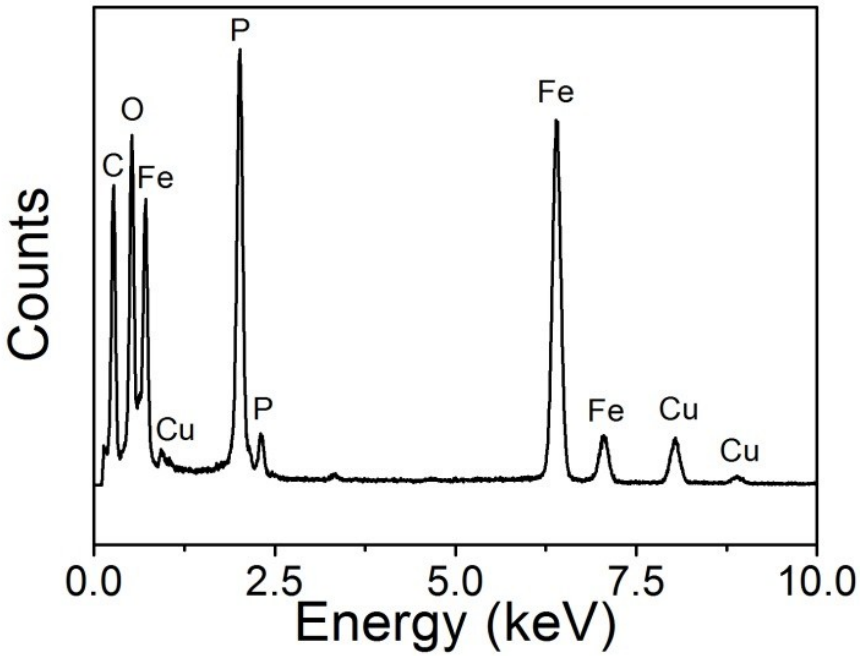

Fig. S4. The EDX spectrum of FePNRs/VAGNs/CC.

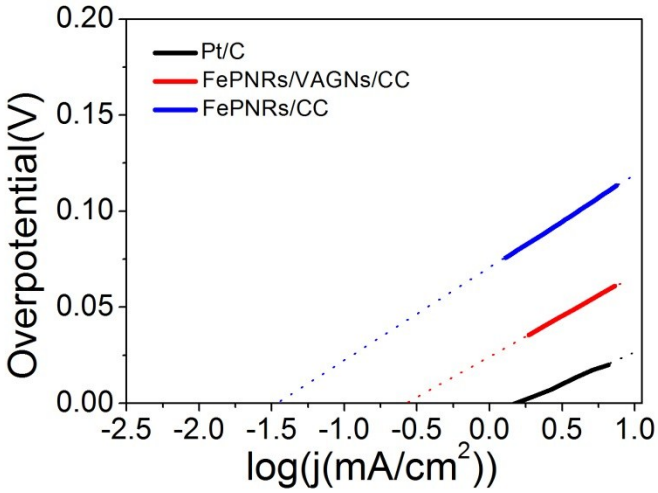

Fig. S5. The Exchange current densities for HER of Pt/C, FeNRs/VAGNs/CC and FePNRs/CC.

Table S2. The comparison of the onset potential, η_{10}, Tafel slope and loading amount of FePNRs/VAGNs/CC in this work and other HER electrocatalysts, including different improvement approaches of FeP and their carbon or other element composites, other noble-metal-free materials and those built on the graphene. ("~" means that the values are our estimation based on the reported data; "-" indicates that

the values are not able to be extracted from the reported papers)

Type	Material or structure feature	Onset potential (mV)	Overpotential at 10 mA cm^{-2} (η_{10}) (mV)	Tafel slop (mV/dec)	Loading amount (mg/cm^2)	Ref.
FeP material	FeP nanoparticles on graphene	~38	123	50	-	S1
	FeP nanorod arrays	20	58	45	1.5	S2
	FeP nanoparticles	50	154	65	-	S3
	Nanoporous FeP nanosheets	~100	~230	67	-	S4
	FeP nanorod on Ti	65	85	60	-	S5
	Carbon-coated FeP microcubes	25	115	56	6.13	S6
	FeP nanowires	~40	96	39	60	S7
	FeP active sites bond carbon nanowires networks	131	256	75.8	-	S8
	Modifying candle soot with FeP nanoparticales	38	112	58	0.28	S9
Our work	FePNRs/VAGNs/CC	19	53	42	0.776	
FeP combining with other element	$Fe_xCo_{1-x}P$ nanowire	-	37	30	-	S10
	$Fe_{0.43}Co_{0.57}S_2$	~125	-	55.9	0.037	S11
	FeP-CoP nanoarray	-	78	75	1.03	S12
Other materials	MoS_2 monolayer	~100	183	77.6	-	S13
	$CoSe_2$ nanowires	~80	130	32	1.3	S14
	WP nanorod	~80	130	69	-	S15
	Ni_2P nanoparticles	~80	~120	87	0.38	S16
	CoP nanowires	~50	110	54	0.35	S17
	MoS_2/Graphene nanosheets	30	110	67.4	-	S18
	WO_2-carbon nanowires	~30	58	46	0.35	S19
	WP_2 nanowire	~70	109	56	-	S20
Other materials on graphene	MoS_2 nanosheets on graphene supported by CC	50	78	53	0.16	S21
	Co_2P nanoparticles on N,P doped graphene	45	103	58	-	S22
	MoS_x on graphene supported by 3D Ni foams	~100	~140	42.8	-	S23
	Nano-nickel on graphene	~50	~100	54	-	S24
	MoS_2 nanoparticles on reduced graphene oxide	~80	150	41	-	S25
	WS_2 on graphene oxide	~150	260	58	-	S26

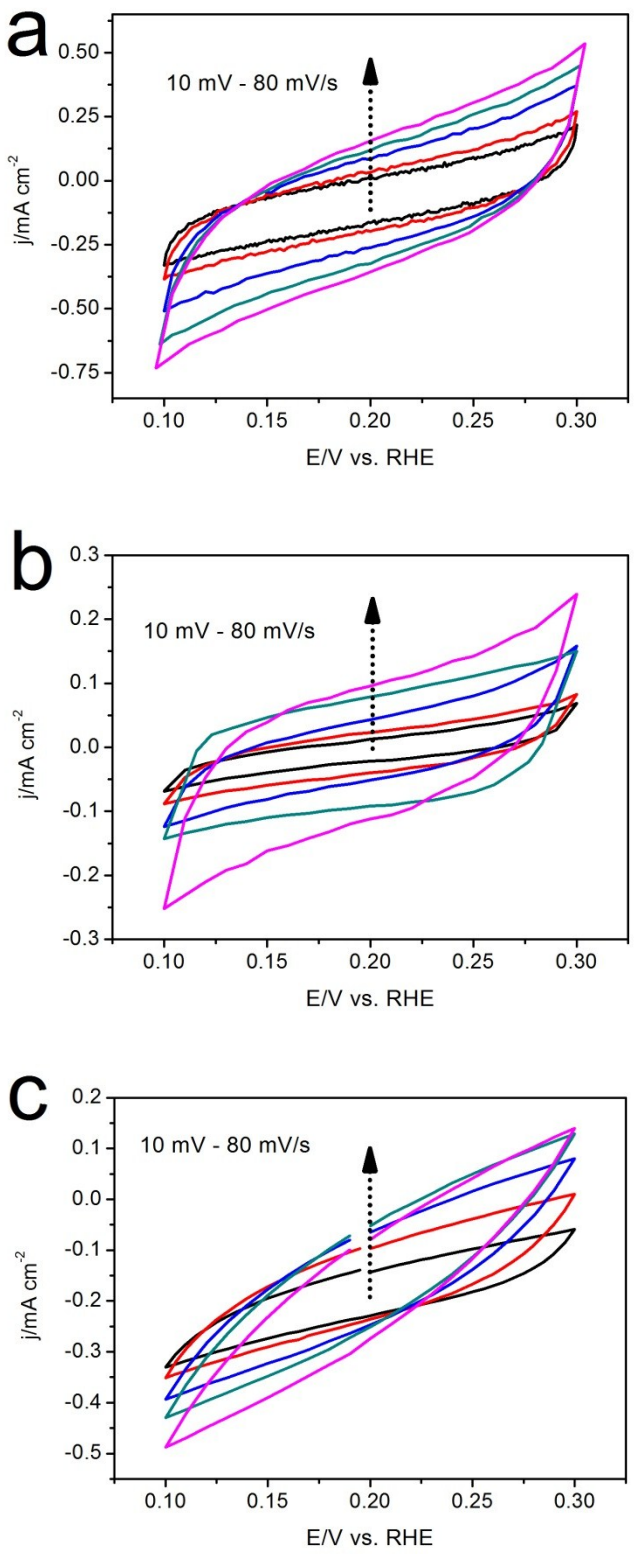

Fig. S6. The cyclic voltammograms with the scan rate of 10, 20, 40, 60, 80 mV/s within 0.1 to 0.3 V of (a) FePNRs/VAGNs/CC, (b) FePNRs/ CC and (c) VAGNs/CC.

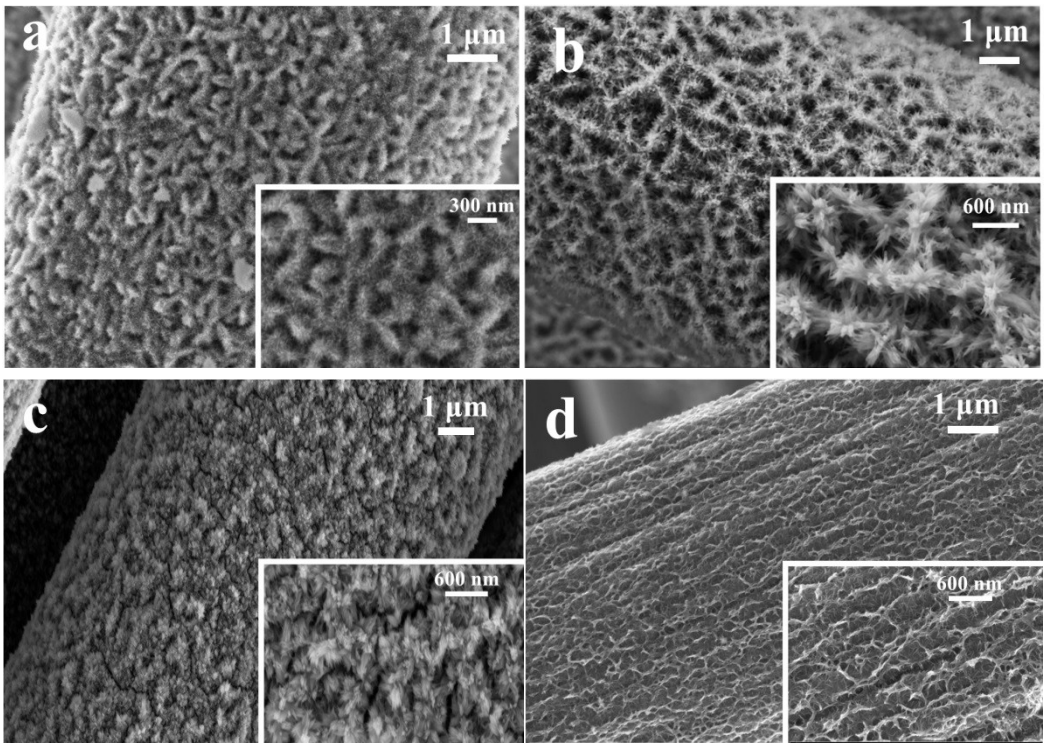

Fig. S7. Low- and high-magnification SEM images of FePNRs/VAGNs/CC samples prepared by different electro-deposition voltage: (a) 0.8 V (FePNRs/VAGNs/CC - 0.8), (b) 1.6 V (FePNRs/VAGNs/CC-1.6 V), (c) 2.4V (FePNRs/VAGNs/CC-2.4) and (d) 3.2 V (FePNRs/VAGNs/CC-3.2).

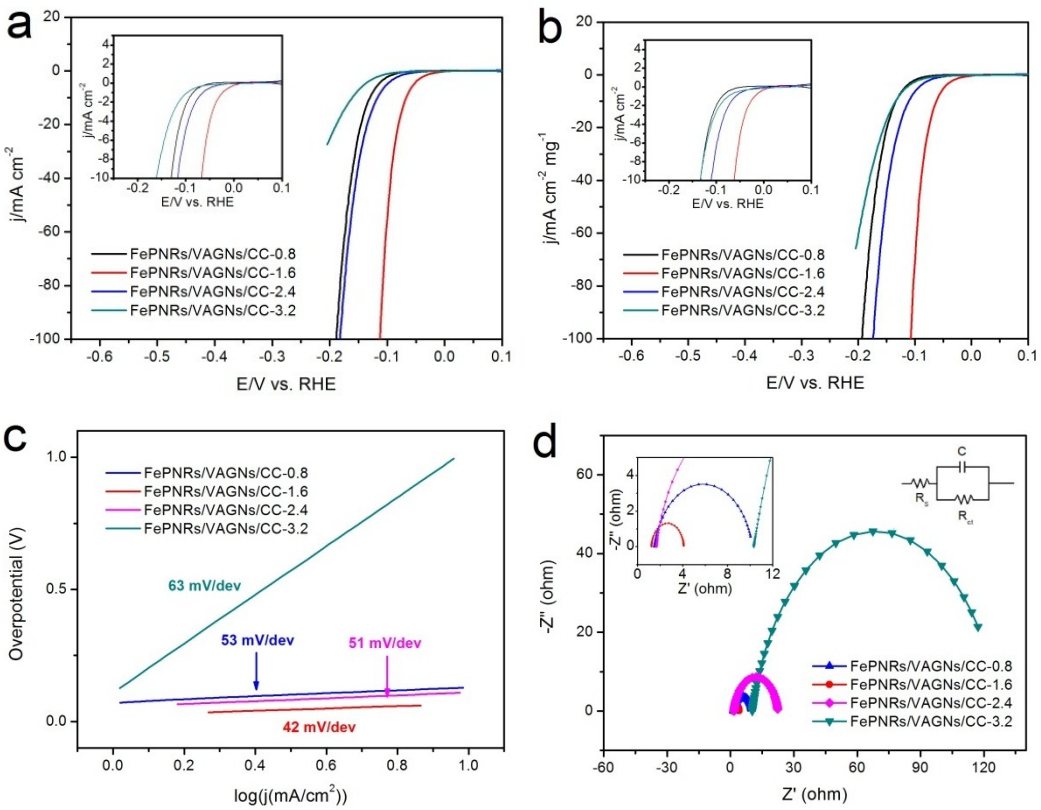

Fig. S8 (a) The polarization curves with the corresponding (b) transformation of polarization curves against unit mass per unit area, (c) Tafel plots and (d) Nyquist plots of as-prepared FePNRs/VAGNs/CC-0.8, FePNRs/VAGNs/CC-1.6, FePNRs/VAGNs/CC-2.4 and FePNRs/VAGNs/CC-3.2. The inset in (a) show the enlargement near the η_{10} region. The insets in (d) show the enlargement of the FePNRs/VAGNs/CC-1.6 and the equivalent circuit used to fit the impedance spectra in which the R_s, R_{ct}, and C represent the electrolyte resistance, electro-transfer resistance, and the chemical capacitance, respectively. The loading amount of FePNRs/VAGNs/CC-0.8, FePNRs/VAGNs/CC-1.6, FePNRs/VAGNs/CC-2.4 and FePNRs/VAGNs/CC-3.2 samples was measured to be 1.159, 0.776, 0.775, 0.4 mg cm^{-2} by ICP, respectively.

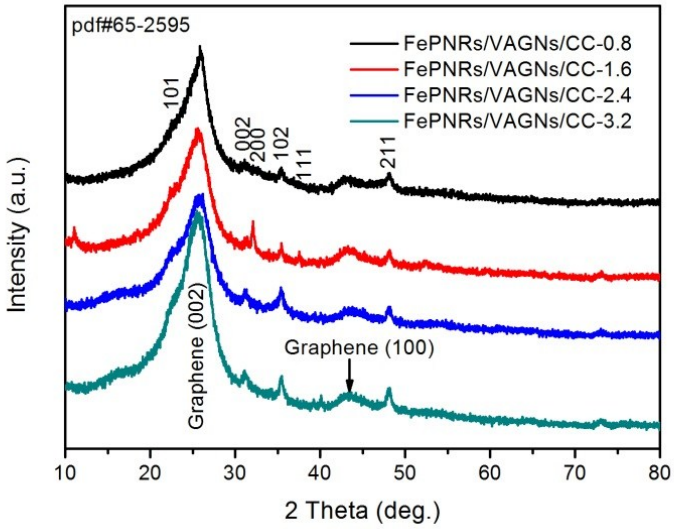

Fig. S9. The XRD pattern of FePNRs/VAGNs/CC prepared by different electro-deposition voltage with the label of standard crystallographic spectrum of FeP (pdf#65-2595).

Reference

[S1] Z. Zhang, B. P. Lu, J. H. Hao, W. S. Yang, J. L. Tang, Chem. Commun, 2014, 50, 11554-11557.

[S2] Y. H. Liang, Q. Liu, A. M. Asiri, X. P. Sun, Y. L. Luo, ACS catal., 2014, 4, 4065-4069.

[S3] L. H. Tian, X. D. Yan, X. B. Chen, ACS catal., 2016, 6, 5441-5448.

[S4] Y. Xu, R. Wu, J. F. Zhang, Y. M. Shi, B. Zhang, Chem. Commun., 2013, 49, 6656-6658.

[S5] R. Liu, S. Gu, H. Du, C. M. Li, J. Mater. Chem. A., 2014. 2. 17263-17267.

[S6] X. Zhu, M. Liu, Y. Liu, R. Chen, Z. Nie, J. Li, S. yao, J. Mater. Chem. A., 2016, 4, 8974-8977.

[S7] C. Y. Son, I. H. Kwak. Y. R. Lim, J. Park, Chem. Commun. 2016, 52, 2819-2822.

[S8] M. Li, T. Liu, X. Bo, M. Zhou, L. Guo, S. Guo, Nano energy, 2017.

[S9] Z. Zheng, J. Hao, W. Yang, B. Lu, J. Tang, Nanoscale, 2015, 7, 4400-4405.

[S10] C. Tang, L. Gan, R. Zhang, W. Lu, X. Jiang, A. M. Asiri, X. Sun, J. Wang, L. Chen, Nano Lett., 2016, 16, 6617-6621.

[S11] D. Kong, J. J. Cha, H. Wang, H. R. Lee, Y. Cui, Energy Environ. Sci., 2013, 6, 3553-3558.

[S12] C. Tang, R. Zhang, W. Lu, L. He, X. Jiang, A. M. Asiri, X. Sun, Adv. Mater., 2017, 29, 1602441.

[S13] C. C. Cheng, A. Y. Lu, C. C. Tseng, X. Yang, M. N. Hedhili, M. C. Chen, K. H. Wei, L. J. Li, Nano Energy, 2016, 30, 846-852.

[S14] Q. Liu, J. Shi, J. Hu, A. M. Asiri, Y. Luo, X. Sun, ACS Appl. Mater. Interfaces, 2015, 7, 3877-3881.

[S15] Z. Pu, Q. Liu, A. M. Asiri, X. Sun, ACS Appl. Mater. Interfaces, 2014, 6, 21874-21879.

[S16] L. Feng, H. Vrubel, M. Bensimon, X. Hu, Phys. Chem. Chem. Phys., 2014, 16, 5917-5921.

[S17] P. Jiang, Q. Liu, C. Ge, W. Cui, Z. Pu, A. M. Asiri, X. Sun. J. mater. Chem. A, 2014, 2, 14634-14640.

[S18] L. Ma, Y. Hu, G. Zhu, R. Chen, T. Chen, H. Lu, Y. Wang, J. Liang, H. Liu, H. Liu, C. Yan, Z. Tie, Z. Jin, J. Liu, Chem. Mater., 2016, 28, 5733-5742.

[S19] R. Wu, J. Zhang, Y. Shi, D. Liu, B. Zhang, J. Am. Chem. Soc., 2015, 137, 6983-6986.

[S20] M. Pi, T. wu, D. Zhang, S. Chen, S. Wang, Nanoscale, 2016, 8, 19779-19786.

[S21] Z. Zhang, W. Li, M. F. Yuen, T. W. Ng, Y. Tang, C. S. Lee, X. Chen, W. Zhang, Nano Energy, 2015, 18, 196-204.

[S22] M. Zhuang, X. Ou, Y. Dou, L. Zhang, Q. Zhang, R. Wu, Y. Ding, M. Shao, Z. Luo, Nano Lett., 2016, 16, 4691-4698.

[S23] Y. Chang, C. Lin, T. Chen, C. Hsu, Y. Lee, W. Zhang, K. Wei, L. Li, Adv. Mater., 2013, 25, 756-760.

[S24] K. N. Mahale, S. T. Ingle, Energy, 2016.
[S25] Y. Li, H. Wang, L. Xie, Y. Liang, G. Hong, H. Dai, J. Am. Chem. Soc., 2011, 133, 7296-7299.
[S26] J. Yang, D. Voiry, S. J. Ahn, D. Kang, A. Y. Kim, M. Chhowalla, H. S. Shin, Angew. Chem. Int. Ed., 2013, 52, 13751-13754.